이학석사학위논문

An Index for Classification of Cold Surge Types over East Asia and its Application to CMIP5 Results

동아시아 한파를 분류하는 지수의 고안과 CMIP5 결과에 적용

2015년 2월

서울대학교 대학원

지구환경과학부

허진우

An Index for Classification of Cold Surge Types over East Asia and its Application to CMIP5 Results

동아시아 한파를 분류하는 지수의 고안과 CMIP5 결과에 적용

지도교수 허 창 회

이 논문을 이학석사학위논문으로 제출함

2015년 2월

서울대학교 대학원

지구환경과학부

허 진 우

허진우의 석사학위논문을 인준함

2015년 2월

위 원 장 _____ (인)

부 위 원 장 _____ (인)

위 원 _____ (인)

Abstract

An Index for Classification of Cold Surge Types over East Asia and its Application to CMIP5 Results

Jin-Woo Heo

School of Earth and Environmental Sciences

The Graduate School

Seoul National University

The cold surges over East Asia can be classified into wave-train type and blocking type according to their dynamic feature. Two indices are introduced to classify the wave-train and blocking type cold surge in this study. The indices capture upper atmosphere pattern, wave-train and meridional dipole structure using potential temperature on 2 potential vorticity

units (PVU) surface. The wave-train index (WI) is defined a difference of anomalous potential temperature on 2 PVU between western North Pacific and northeast china to capture the wave-train, trough-ridge pattern. The blocking index (BI) is defined a difference of anomalous potential temperature on 2 PVU between subarctic region and northeast china to capture blocking pattern, meridional potential temperature gradient reversal. The each cold surge classified by the index method have essential feature in observation. The wave-train type has baroclinic wave with southeastward

Siberian high expansion and the blocking type has dipole structure indicating the subarctic blocking and deepening of East Asian coastal trough induces a southward expansion of the Siberian high. The blocking type cold surge is less frequent but stronger and longer than the wave-train type cold surge. In addition, we exclude the cold surge don't have the wave-train and dipole structure.

The index method is applied to 13 CGCMs in CMIP5. In historical run the cold surges in 13 CGCMs is well classified into the wave-train and blocking type cold surge by the index method. Wave-train type has wave pattern, and blocking type has dipole pattern in historical run. However, many 13 CGCMs simulate the less occurrence of cold surge and stronger and longer in both types in historical run compared with observation results. In RCP8.5, the ensemble mean occurrence and intensity of both types decreases, and the duration increases in blocking type, decreases in wave-train type.

Key words: Cold surge, East Asia, Classification, CMIP5

Student Number: 2013-20348

Table of Contents

List of figures

List of Tables

1. Introduction

The cold surge over East Asia is defined by abrupt temperature drop within 1 or 2 days with intra-seasonal amplification of Siberian High. In East Asia, it is known that the temperature drop is followed by an expansion of Siberian High which induces cold advection with northerly wind sustaining along flank of Siberian High. Hence, it often results in socioeconomic impacts on East Asia countries (e.g., China, Japan, and Korea). There are approximately ten cold surges over East Asia a winter (Chen et al., 2004) and it sometimes accompanies snowfall and freezing precipitation. The cold surge sometimes produces anomalous convective activity off South China Sea (Chen et al., 2002) and influences on remote area, North America (Cohen et al., 2001).

The most widely known dynamic mechanism to cause intra-seasonal Siberian High amplification associated with generating and maintaining the East Asian cold surge is the propagation of wave-train in upper-troposphere from Europe to Asia (Takaya and Nakamura 2005a). The disturbances over Eurasian continent grow before Siberian High amplification. The disturbances (i.e., trough-ridge pattern) grow into a wave-train which propagates southeastward to deepen climatological trough over East Asian seaboard. The northwesterly wind induced by the trough brings the pre-existing cold air over Siberian high (Joung and Hitchman 1982; Zhang et al. 1997). The cold advection amplifies the Siberian High and further induces vorticity advection which reinforces the anticyclonic and cyclonic circulation which forms the upper-tropospheric wave-train (Chen et al. 2002). In conclusion, the wave-train over Eurasia is important to generating and sustaining cold surges over East

Asia with the Siberian high and pre-existing cold anomaly over Siberia (Takaya and Nakamura 2005a).

On the other hand, Takaya and Nakamura (2005b) reported other mechanism of Siberian High amplification. The subarctic blocking is another mechanism to generate cold surge. They suggested anticyclonic blocking caused by strong feedback forcing from Pacific storm track can initiate cold surge with the intra-seasonal Siberian high amplification through composite analysis of 20 strongest Siberian High events. According to Park et al (2008), retrograding anticyclonic blocking observed from surface to stratosphere modulates troposphere to produce favorable condition for Siberian high amplification. Park et al. (2010) reported blocking cold surges led to long-lasting cold weather and heavy snowfall with with large-scale variability, such as the Arctic Oscillation and the Madden-Julian Oscillation.

Recently, Park et al. (2014) classified cold surges using an agglomerative hierarchical clustering method during cool season (NDJFM) in the period 1954/55-2005/06 and analyzed dynamical characteristics of two cold surge types. The classification of cold surges by clustering method is successful and captures the characteristics of previous study but clustering method just use Euclidean distance, statistical similarities, between samples to classify the cold surge without any dynamical bases. Accordingly the result by clustering method may be different with periods. For example, it is possible the same cold surge is classified into different type with respect to a target period because the clustering procedure does classification all over again. Especially the cold surge has both wave-train and blocking feature is sensitive to clustering criteria which makes clustering method

unstable. For this reason we need to use fixed index to capture dynamical patterns.

The previous studies about the cold surge over East Asia focused on the entire cold surge, not two types, in future climate such as Park et al. (2011). They investigated only the frequency of entire cold surge and cold day in the future climate and reported the frequency of cold surge declines. However change of other characteristics such as duration and intensity is important in the future climate. Also, we should consider the wave-train and blocking type which have different feature.

This paper is organized as follows. Section 2 describes the data used and Section 3 provide the cold surge definition and the problem of clustering method also introduces the indices to classify the wave-train type and blocking type based on dynamical feature. In section 4, we show the distinct feature of two cold surge type using the new indices in observation. Next, the cold surges simulated in historical run in CMIP5 are classified by the new indices and we confirm whether the indices classify cold surges properly. The same procedure is performed under RCP8.5 and we show that the change of the cold surge in the future climate. Section 5 gives a summary and discussion.

2. Data & Methods

To detect cold surge occurrence dates we use daily 2m temperature (T2m), mean Sea Level Pressure (SLP) from European Center for Medium-Range Weather Forecasts (ECMWF) Re –Analysis Interim (ERA-interim) (Dee et al., 2011), which have a horizontal resolution of 1.5°×1.5 in addition to potential temperature on 2 Potential Vorticity Unit (2PVU) to define Wave-train (WI) and Blocking (BI). Geopotential at 300 hPa, 850 hPa are used to compare spatial patterns between observation and CMIP5 output. Observation period is 1979/1980 to 2010/11.

To verify the performance of the model for simulating two types of cold surge. We use T2m, SLP, geopotential in 14 models (ACCESS1-0, ACCESS1-3, BNU-ESM, CanESM2, CMCC-CESM, CMCC-CMS, CNRM-CM5, CSIRO-Mk3-6-0, GFDL-ESM2G, IPSL-CM5A-LR, IPSL-CM5A-MR, MPI-ESM-LR, MPI-ESM-MR, NorESM1-M) belong to CMIP5 under historical run and RCP8.5. We also use zonal wind, meridional wind, and temperature, which have several pressure levels to estimate potential temperature on 2PVU. Table 1 shows detailed model descriptions.

Model	Origination Group	Country of Origin	Atmospheric Resolution
ACCESS1-0	CSIRO & BOM	Australia	N96L38
ACCESS1-3	CSIRO & BOM	Australia	N96L38
BNU-ESM	BNU	China	T42L26
CanESM2	CCCMA	Canada	T63L35
CMCC-CESM	CMCC	Italy	T31L39
CMCC-CMS	CMCC	Italy	T63L95
CNRM-CM5	CNRM	France	TL127L31
GFDL-ESM2G	GFDL	USA	2.5° × 2.0°L24
IPSL-CM5A-LR	IPSL	France	1.9° × 3.75°L39
IPSL-CM5A-MR	IPSL	France	1.25° × 2.5°L39
MPI-ESM-LR	MPI	Germany	T63L47
MPI-ESM-MR	MPI	Germany	T63L95
NorESM1-M	NCC	Norwegia	1.9° × 2.5°L26

Table 1. Description of the Coupled Global Climate models used in This Study

3. Cold surge definition and Classification

3.1. Cold surge definition

Siberian high expansion and abrupt drop in the SAT within 1 day or 2 days are the important parts to define cold surge occurrence. To capture both characteristics previous studies regard the absolute day-to-day SAT drop and mean SLP over Siberian high (e.g. exceeds 1035 hPa) as cold surge criteria (Chen et al, 2004). Similarly, the recent studies (Jeong and Ho 2005; Park et al. 2011; Woo et al. 2012; Park et al 2014) employed a regional intra-winter variability instead of the absolute value as SAT drop criterion and SLP in center of Siberian high. We choose similar criteria which Park et al. (2014) used.

At first, SAT drop exceeds 1.5 σ (standard deviation of the daily SAT in all cool season) over Northeast China (40°N-45°N, 120°E-125°E) or Korea peninsula (35°N-40°N, 125°E-130°E). Because cold surges over East Asia are synoptic phenomena those two domains are enough to capture the cold surge which influences on East Asia and to exclude temperature drop due to radiative local cooling. Second, the SLP in anticyclonic center of Siberian high domain (90°E-115°E, 35°N-55°N) exceeds 1030 hPa, because intra-seasonal Siberian high amplification is the most important part of cold surge occurrence. The center of anticyclone is defined as a point in which geopotential at 1000 hPa is larger than the value of near 8-point (Zhang and Wang 1997). The domains used in this study are represented in Figure 1. However we use mean sea level pressure in CMIP5 because some CMIP5 models don't provide geopotential at 1000 hPa. Third, surface temperature anomaly is less than 0 to remove warm cold surges. The cold surge termination day is defined by the daily

SAT anomaly larger than -0.5 σ. When we choose 0 SAT anomaly as criterion, there are unrealistic cold surge which have duration more than 30 days.

There are 352 cold surges using above criteria during 32 winters. It means that 2.2 cold surge event occurs per month. This is higher than the number of cold surge occurrence reported by Zhang et al. (1997), Jeong and Ho (2005), and Woo et al. (2012), 1.85, 1.40, and 1.56 per month respectively. Above criteria detect too many cold events, because it capture local signal which is not typical large-scale circulation signal. To exclude these local cold event we used two indices as one of criteria. These new indices are based on dynamical feature of cold surges and we classify cold surge using these indices.

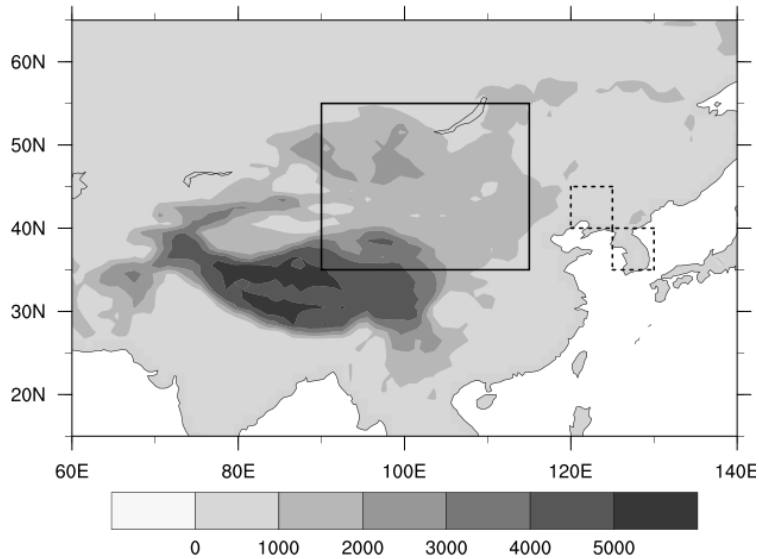

Figure 1. Siberian high domain (solid lines), North-east china and Korean peninsula domain (dotted lines). Shading indicates topography

3.2 Clustering method for classification of the cold surge

Park et al. (2014) used agglomerative hierarchical clustering to 300 hPa geopotential anomalies (raw daily geopotential minus climatology) when cold surges occur to classify cold surge over 60°E–180°E and 20°N–90°N where the main feature of the wave-train and blocking type is observed. In this method, each geopotential at 300 hPa pattern is regarded as a vector. After obtaining vector, the cluster number decreases in each step to emerge the most two similar clusters into one cluster using Ward's minimum variance clustering criterion (Kalkstein et al. 1987). When there are N clusters, the average of squared sum of differences between objects which constitute one cluster in m^{th} cluster is defined as the error sum of squares (ESS_m) and sum of the error sum of squares in N clusters is defined as total error sum of squares ($TESS_N$). We find a pair of cluster which minimizes the difference between $TESS_N$ and $TESS_{N-1}$. It indicates that the most similar two clusters merged into new one cluster. Repeating this process, we terminate it before the greatest increase appear, which means the most different clusters merged. According to above criteria we terminate at final step. Using clustering classification method, cold surges are classified into two groups, 284 and 68 cold surges in the wave-train type.

However, the clustering method just uses statistical criteria, Euclidean distance, and it is possible that the same cold surge can be classified into other cluster with respect to the group of samples. For example, we conduct the clustering method for period 1 (1979-2011) and period 2 (1979-1989) and identify what type the cold surge is classified to during period 1. Some cold surge have other type with respect to the period (not shown). The clustering procedure initiate totally at first when period

changes so the results is sometimes very different between other periods. Especially the mixed type which has the wave-train and blocking patterns is critical the different results. When clustering method is terminated before final step the number of clustering is 3. One has the wave-train type pattern, other does the blocking type pattern, and another cluster, mixed type, has both patterns. The mixed type makes above difference. The clustering method doesn't provide absolute classification so we develop the index method which is fixed criteria.

3.3 Two indices for classification of the cold surge

Pelly and Hoskins (2003) invented a new index to capture Northern Hemisphere blockings. They used meridional gradient of potential temperature on 2PVU, dynamic tropopause. The potential temperature is a good tracer in frictionless and adiabatic conditions, hence there are advantages in tracing air mass related to the extratropical synoptic condition. We employ this method to capture the wave-train and blocking patterns with modification. It catches dynamical feature and makes up shortcoming of clustering method.

Figure 2 shows schematic feature of two type in geopotential at 300 hPa. There is south-eastward wave-train (ridge-trough-ridge pattern) from Eurasia to East Asia in Figure 2a in which negative anomaly is located in Northeast China and Korea peninsula with positive anomaly on both side. The pattern is south-north fluctuation of Z, which is associated with equatorward and poleward bending of climatological Z pattern. On the other hand, there is meridonal dipole structure in Figure 2b. Tyrlis and Hoskins (2008) suggested that the cyclonic breaking of Rossby wave asccosiated with such a poleward intrusion of high Z and the equatorward intrusion of low Z. The wave-train (blocking) cold surge is associated with wave propagation (wave breaking).

To capture spatial patterns wave-train and blocking cold surges we invented the wave-train index (WI) and blocking index (BI). Hoskins et al. (1985) suggested that extratropical synoptic disturbance is well approximated in adiabatic motion, so potential temperature on 2PVU which is conserved is good tracer for wave propagation and wave breaking. The wave propagation and breaking is the prominent in baroclinic zone on tropopause. According to Brerisford (1988), 2PVU

surface is referred to the dynamic tropopause. We modify the method of Pelly and Hoskin (2003) to capture wave-train and blocking pattern. Likewise Z pattern, potential temperature on 2PVU in wave-train type shows positive anomaly in central Siberia and Western Pacific and negative anomaly in northeast China and Korea. Also, there is dipole pattern in the case of blocking type.

For wave-train type, there are ridge (trough) in central Siberia and western Pacific (northeast China and Korea). We define wave-train index (WI) to represent this quantitatively. WI is defined as the difference of potential temperature anomaly between western Pacific (R3: 30°N-55°N, 140°E-170°E) and northeast China (R2: 35°N-60°N, 110°E-140°E). In this definition, wave-train type have positive WI. On the other hand, there is not positive anomaly in R3, so blocking type have small WI.

For blocking type, there are positive anomaly in subarctic region and negative in northeast China and Korea. The blocking index (BI) is defined the difference of potential temperature anomaly between subarctic region (R1: 65°N-90°N, 110°E-140°E) and northeast China (R2: 35°N-60°N, 110°E-140°E). The blocking type have positive BI, while wave-train type have small BI. We use two indices to classify cold surge.

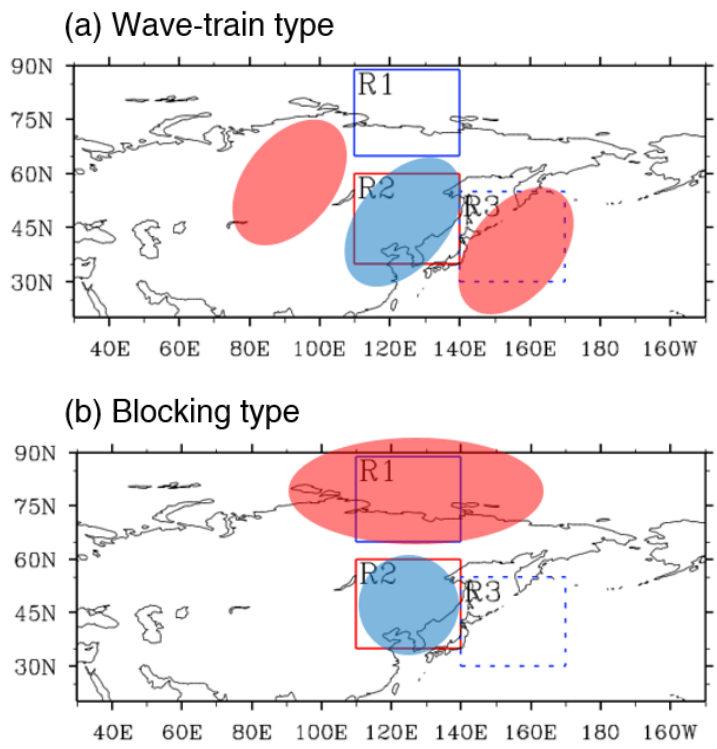

Figure 2. The schematic patterns of (a) wave-train type and (b) blocking type in geopotential at 300 hPa. The domains to define WI and BI. (R1: 65°N-90°N, 110°E-140°E, R2: 35°N-60°N, 110°E-140°E, R3: 30°N-55°N, 140°E-170°E).

4. Result

4.1 Two types of cold surge classified by the new indices in observation

To verify the index method we apply the index method to observation. Figure 3 shows a scatter plot of BI and WI. In Figure 3a, the cold are surge classified with criteria WI > BI indicates the wave-train type, opposite indicates the blocking type and the cold surge which have negative BI and WI is excluded. On the other hand, the result of the clustering method are shown in Figure 3b. In the view of average, the wave-train type classified by the clustering method have positive WI and blocking type shows same result, positive BI. However, their spread is so large and the some wave-train type have blocking pattern the blocking type do too. There are 188 wave-train type and 104 blocking type for analysis period. The occurrence of wave-train type is quite larger than of blocking type.

Figure 4 shows composite maps in the day wave-train and blocking type classified by the index method occur. In figure 4a, c, e, baroclinic wave progress from northwest to southeast. In Figure 4b, d, f, there are barotropic positive geopotential anomaly over subarctic and meridional dipole structure. Also, vertical cross section on the line of Figure 4 are shown in Figure 5. Above mentioned, Figure 5a shows baroclinic wave in which there are west-tilt of geopotential and east-tilt of temperature. In blocking type, Figure 5b, there are barotropic geopotential anomaly in subarctic which reach to above troposphere and meridional dipole structure. Also Figure 6 shows the composite maps of MSLP and anomalous temperature, meridional wind at 850 hPa. In Figure 6a, c, the MSLP progresses south-eastward

likewise the wave-train and anomalous northerly wind produce cold air to Northeast China and Korean Peninsula. In Figure 6b, d, the positive MSLP covers in subarctic and progresses southward. In Figure 6e, f, the wave-train type shows west-northerly wind and the blocking type shows east-northerly wind.

We investigate characteristics such as duration and intensity. The results are in Figure 7. In our study, the intensity is defined the sum of temperature anomaly during cold surge duration. The blocking type is stronger and longer than the wave-train type. Intensity is function of duration so we calculate averaged duration. In averaged duration the blocking type is stronger than the wave-train type.

Above mention, the cold surge which have both negative WI, BI is excluded. To clarify this point we conduct same analysis to excluded cold surge. The composite maps of unclassified cold surge are shown in Figure 7. In Figure 7a, b, the cold core in unclassified cold surge is weaker and it doesn't expand to domain of the cold surge detection but cold core in both wave-train and blocking expands to the domain. In Figure 7c, geopotential at 300 hPa shows significant positive anomaly over East Asia. However, this is not general upper pattern about cold surge occurrence. Also, because the cold surge definition use Siberian high there are positive center over Siberian high. However the intensity is weaker than others. The unclassified cold surge is weaker than the wave-train and blocking cold surge and it doesn't have general upper pattern. It is reasonable to exclude the cold surge which have negative WI and BI.

Because the index method use fixed index to classify the cold surg. various applications are possible. For example the cold surge can be classified into 3 types when we use criteria BI > 2*WI, 2*WI > BI > 1/2*WI, and 1/2*>BI. In that case we

can focus on the association between the wave-train pattern and blocking pattern and purely the wave-train or blocking pattern. Also, the WI (BI) shows significant change before the wave-train (blocking) type cold surge occurs which is used for prediction.

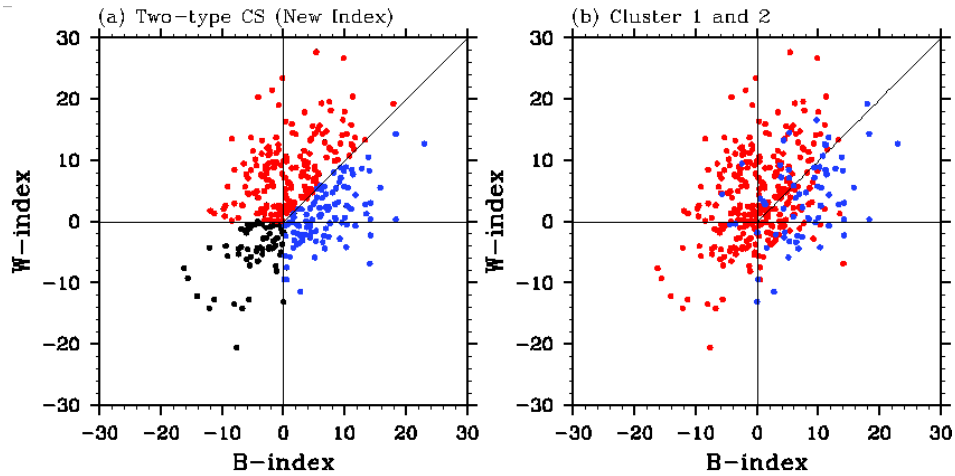

Figure 3. Scatter plots of WI and BI. (a) the wave-train type (red dots), the blocking (blue dots), and unclassified (black dots) are classified by the index method. (b) the wave-train type (red dots) and the blocking type (blue dots) are classified by the clustering method.

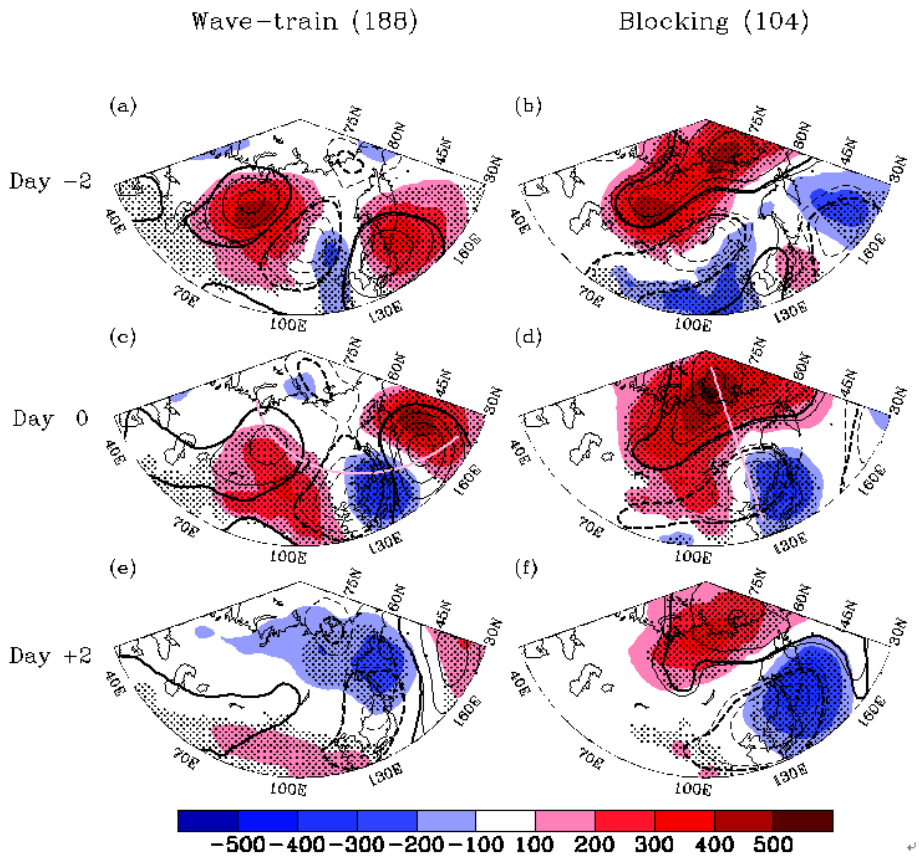

Figure 4. Composite of geopotential at 850 hPa (shading; black dot indicates significantvalues at 95% confidence level) and 300 hPa (contour inverval of 300 $m^2 m^s$; thick contour indicates significant values at 95% confidence level) from day -2 to day +2 relative to cold surge occurrences. The pink line in (c, d) indicate the wave-guided line and the blocking-ridge line.

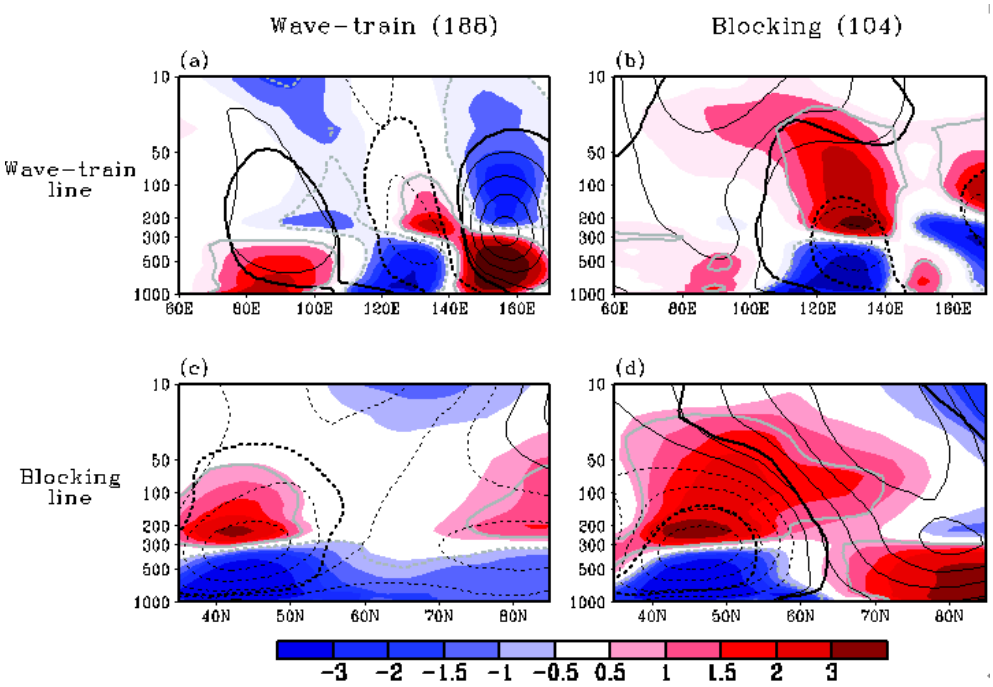

Figure 5. Vertical cross-sections of geopotential anomaly (contour inverval of 300 $m^2 m^s$; thick black line indicates significant values at 95% confidence level) and temperature anomalies (shading; units are K; thick grey line indicates significant values at 95% confidence level). (a, c) is along the line in Fig. 5c and (b, d,) are along the line in Fig. 5d for occurrence day.

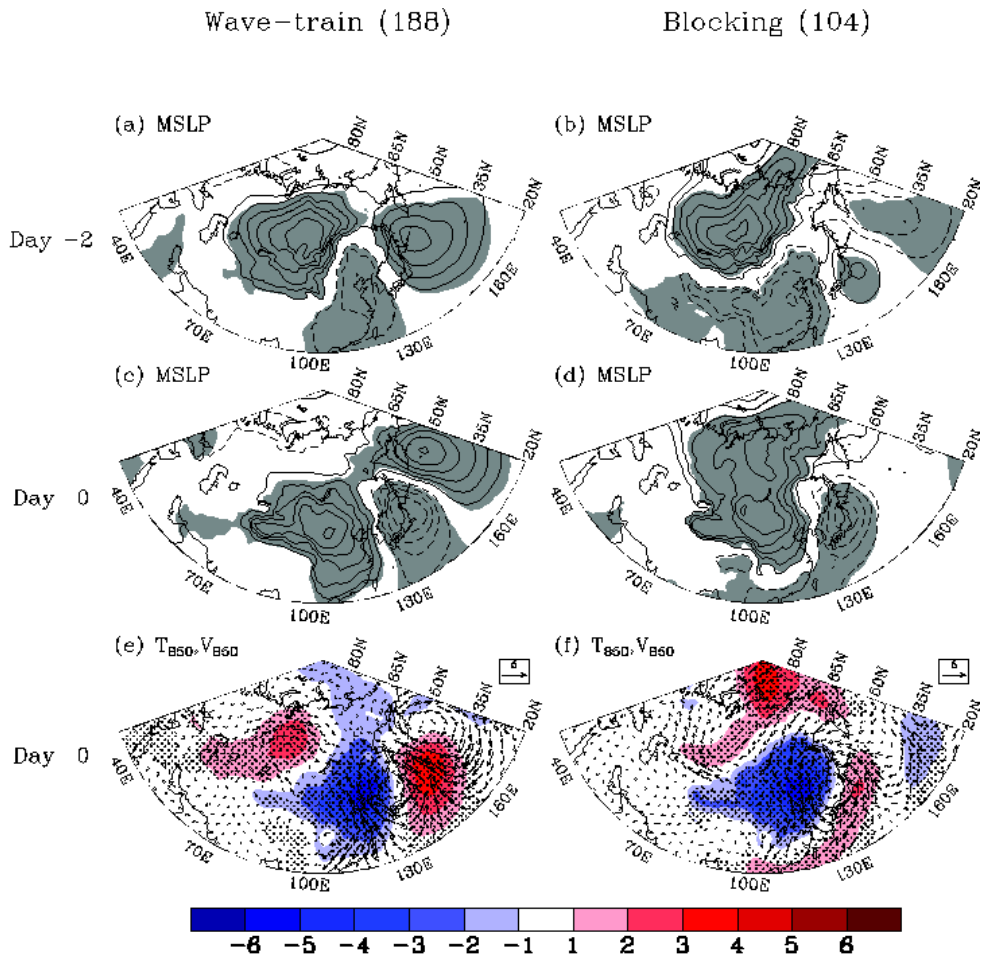

Figure 6. Composite maps of MSLP anomalies (contour interval of 100 hPa; shading indicates significant values at 95% confidence level) in (a, b) for day -2, (c, d) for day 0. Temperature anomaly (shading; black dots indicates significant values at 95% confidence) and wind anomalies (vector) at 850 hPa in (e, f) in the occurrence day.

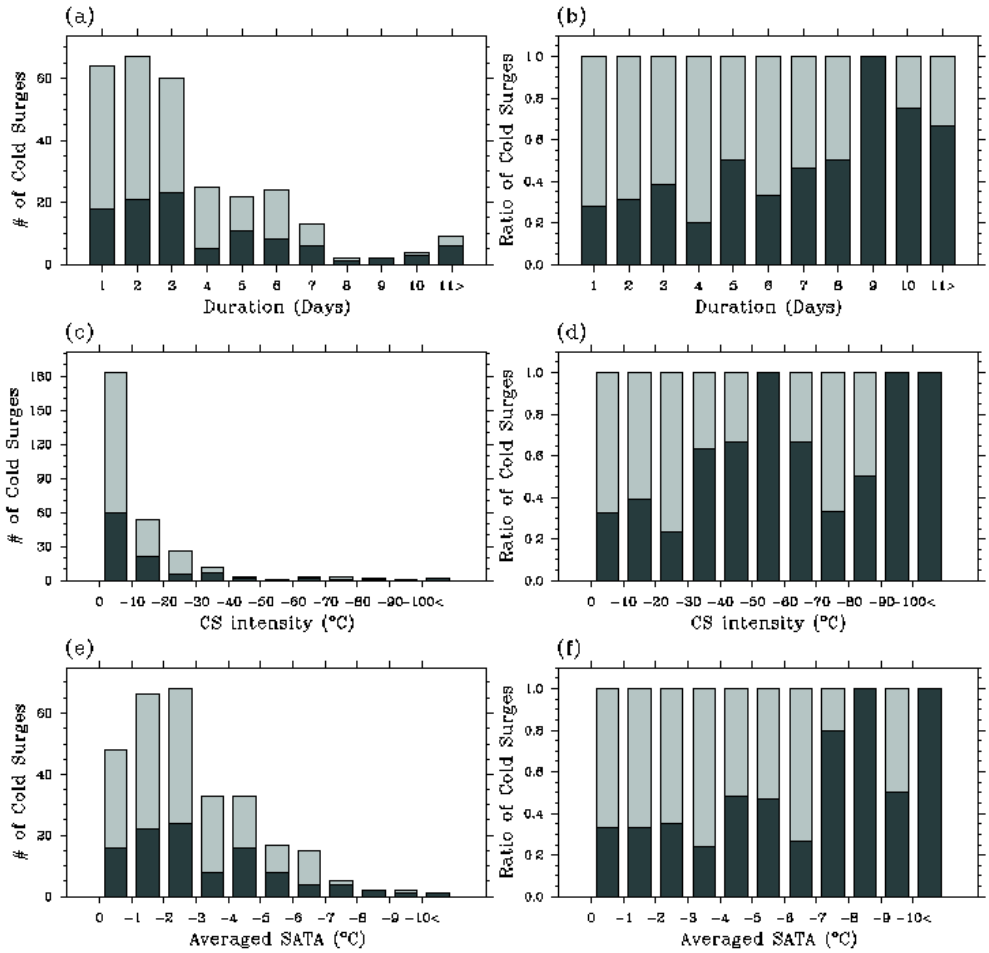

Figure 7. The number of cold surge occurrence day of wave-train (light grey) and blocking (dark grey) types in the left panels. The right panels show their ratio. The duration is in (a, b). The intensity is in (c, d) and SAT anomalies averaged over their durations in (e, f).

4.2. Validation for cold surge classification by the index method in CMIP5

Prior to analyzing the change of the cold surge in future climate we validate how two types of cold surge are classified by the index method. Figure 8 shows composite maps in the day wave-train and blocking occur. There is a west-tilt of geopotential, baroclinic wave, in observation. All wave-train type cold surges simulated by 13 CGCMs have west-tile structure, baroclinic wave, which processes south-eastward (not shown). On the other hand, figure 9 shows composite maps in the day the blocking type cold surge occurs. In observation barotropic positive geopotential anomaly and meridional diploe structure is key features. 13 CGCMs simulate the features of blocking type cold surge. In the view of spatial structure the index method successfully classifies cold surges simulated by CGCMs into two types. However, the magnitude of center is little stronger in CGCMs than observation.

The characteristics of two types of the cold surge such as intensity, duration are investigated to validate how well CGCMs simulate the cold surge. The blocking type is stronger and longer but the wave-train type is more frequent in observation. We confirm those features in CGCMs. The characteristics of the cold surge simulated by CGCMs in historical run are shown in Table 2. All CGCMs simulate less the occurrence day than observation in both types. A ratio of the occurrence day (W/B) is 1.81 in observation which is very similar with the ratio from CGCMs. Many CGCMs simulate longer duration in the wave-train (blocking) type except CanESM2, CMCC-CMS, CNRM-CM5 (BNU-ESM, CMCC-CESM, CNRM-CM5, IPSL-CM5-LR). There is no CGCM which simulate weaker cold surge because the winter

temperature anomaly in the cold surge definition is larger in CGCMs. There are bias in the duration and intensity but they simulate the blocking type is stronger and longer. In conclusion, CGCM successfully simulate the cold surge qualitatively.

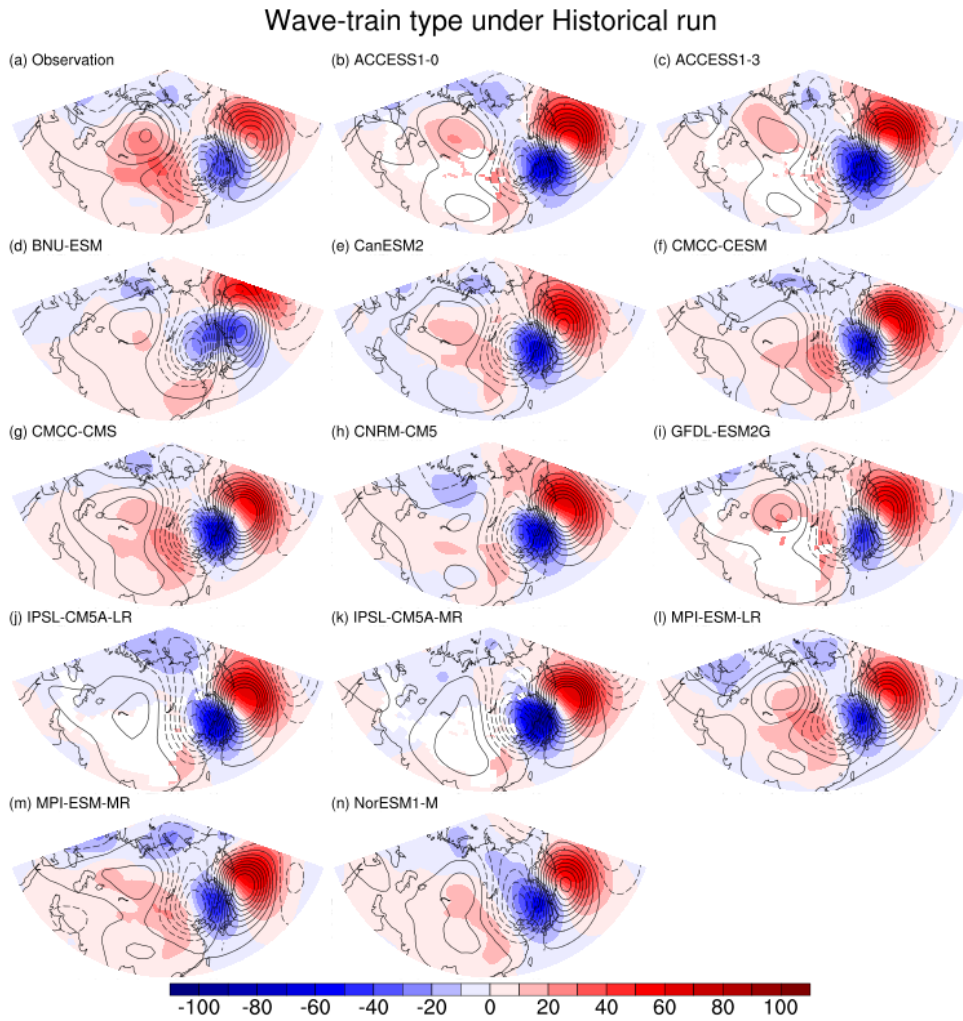

Figure 8. Composite of geopotential height amonalies at 300 hPa (countour, in intervals of 20m) and 850 hPa (shaded) in the occurrence day of the wave-train type under historical run.

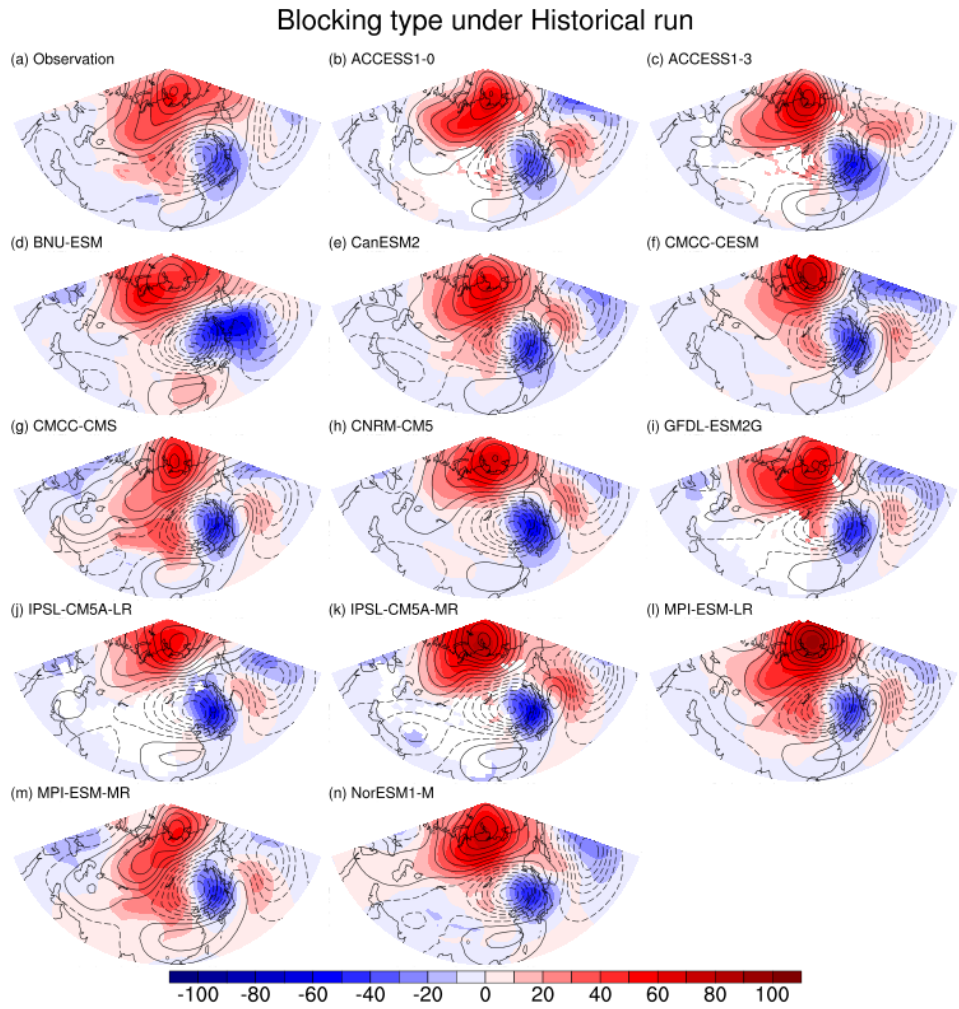

Figure 9. Same as Figure 8 but of the blocking type.

	Occurrence day (/yr)		Duration (day)		Intensity (℃)	
	Wave-train	Blocking	Wave-train	Blocking	Wave-train	Blocking
Observation	5.70	3.15	3.11	4.24	-10.2	-16.3
Ensemble mean	3.96	2.25	3.40	4.40	-16.4	-22.2
ACCESS1-0	3.38	1.95	3.75	4.66	-16.0	-20.7
ACCESS1-3	3.95	2.20	3.91	4.52	-15.1	-18.7
BNU-ESM	5.04	2.69	3.25	3.76	-19.3	-22.2
CanESM2	4.56	2.76	2.93	4.42	-14.7	-25.7
CMCC-CESM	3.98	2.27	3.10	3.89	-13.9	-18.6
CMCC-CMS	3.51	1.87	3.97	4.72	-21.4	-23.7
CNRM-CM5	4.55	2.60	3.02	3.79	-17.5	-22.3
GFDL-ESM2G	4.19	2.44	3.33	4.52	-18.8	-26.4
IPSL-CM5A-LR	3.45	1.73	3.51	4.63	-16.2	-21.8
IPSL-CM5A-MR	3.82	2.22	3.52	4.36	-14.2	-19.7
MPI-ESM-LR	3.49	2.31	3.43	4.83	-15.6	-23.2
MPI-ESM-MR	3.31	2.00	3.30	4.58	-15.7	-23.9
NorESM1-M	4.27	2.22	3.21	4.48	-14.4	-21.5

Table 2. The characteristics of two types of cold surge in observation and CGCMs under historical run.

4.3 The change of the cold surge under RCP8.5

Although the performance of simulating the cold surge is similar in CGCMs under historical run, it is a different problem that the index method works under RCP8.5. The spatial pattern of each cold surge classified by the index method is identified in the early twenty one century (2020-2050) and the late twenty one century (2065-2095). 96 years are too long regarded as one climate so we choose two periods, 2020-2050 and 2065-2095. Figure 10, 11 are composite maps of wave-train and blocking cold surge occurrence day in the early twenty one century. Figure 12, 13 are same as Figure 10, 11 but in the late twenty one century. There is a distinct baroclinic wave in Figure 10 and Figure 12 in all CGCMs. Also there are barotropic negative geopotential height over sub-arctic and meridional dipole structure in Figure 11 and Figure 13 in all CGMCs. All CGCMs simulate well the spatial pattern of two types.

The changes of characteristics in the early and late twenty one century are shown in Figure 14. In Figure 14 (a)-(c), the most noticeable feature is that the occurrence days of both cold surges decreases in the future climate. The change of occurrence days of ensemble mean between historical run and the late twenty one century is -0.50(-0.52) in the wave-train (blocking) type cold surge. On the other hand, there is a small difference between historical run and the early twenty one century. In Figure 14 (d)-(f), the duration of the wave-train type cold surge decreases (-0.19 day) from historical run to the late twenty one century. However, the duration of the blocking type cold surge slightly increases (+0.10 day). The two cold surges have the opposite trend of duration in the climatological aspect. It is careful that inter-model sample standard deviation in the blocking type cold surge is larger in

future climate. In Figure 14 (g)-(i), although two cold surge weaken in the late twenty one century, the magnitude of changes is larger in the wave-train type (+2.18℃) cold surge than the blocking (+1.00℃). It is possible the longer duration makes the intensity stronger so we calculate averaged intensity (i.e. sum of intensity/duration in each cold surge case). The change in the averaged intensity is +0.41℃ (+0.36℃) in the wave-train (blocking) type cold surge.

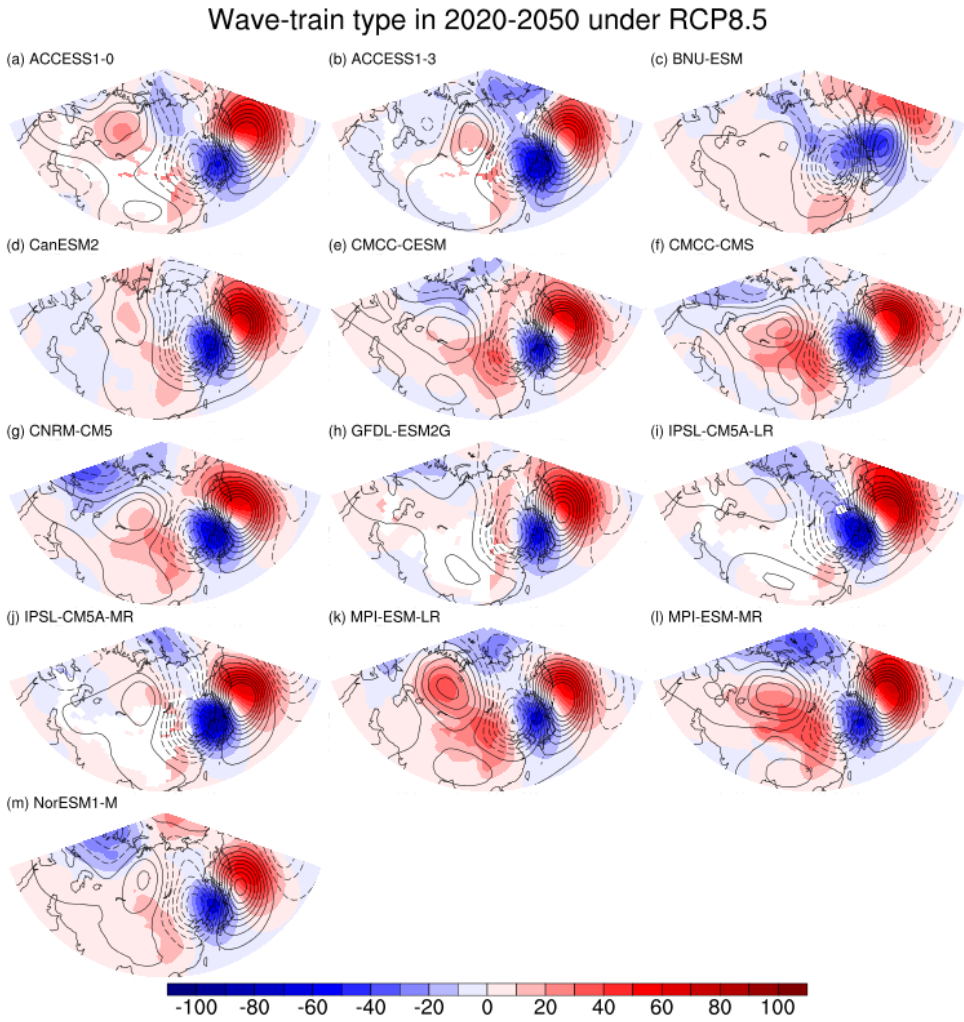

Figure 10. Same as Figure 8 but under RCP8.5 for 2020-2050.

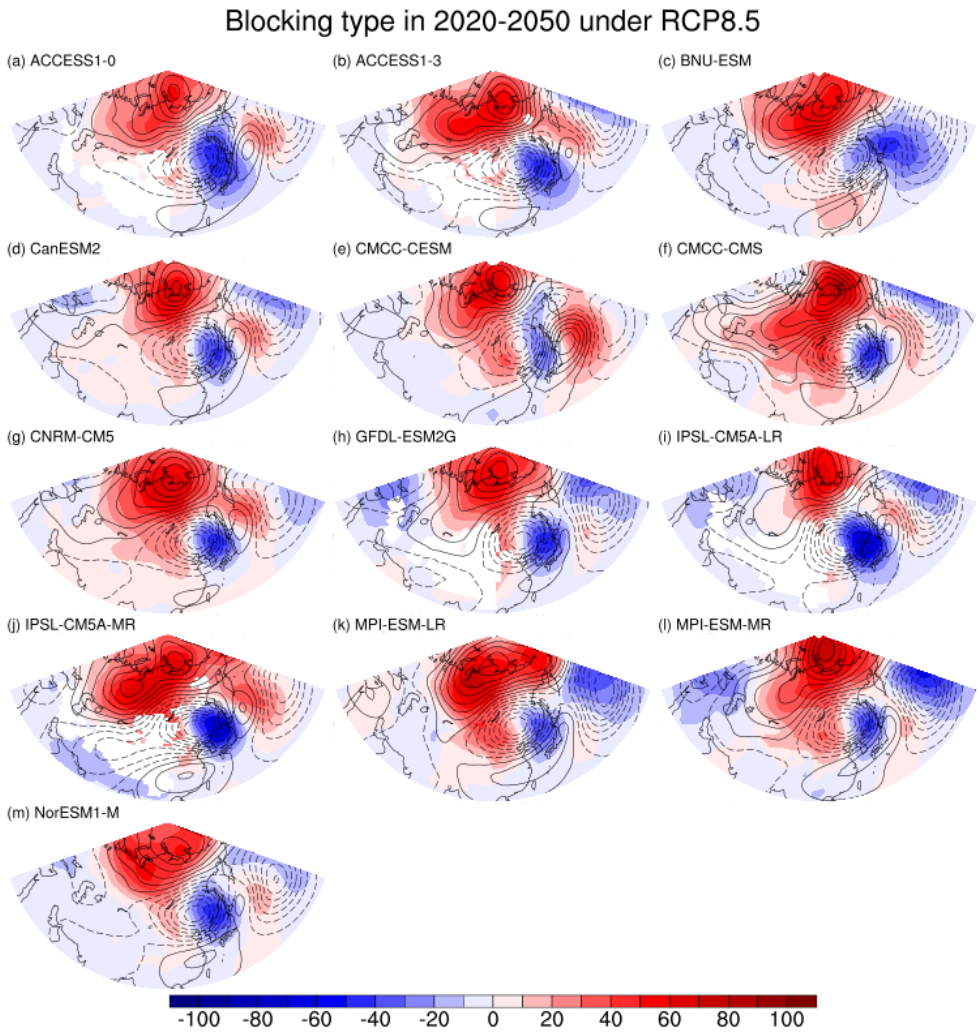

Figure 11. Same as Figure 8 but of the blocking type under RCP8.5 for 2020-2050.

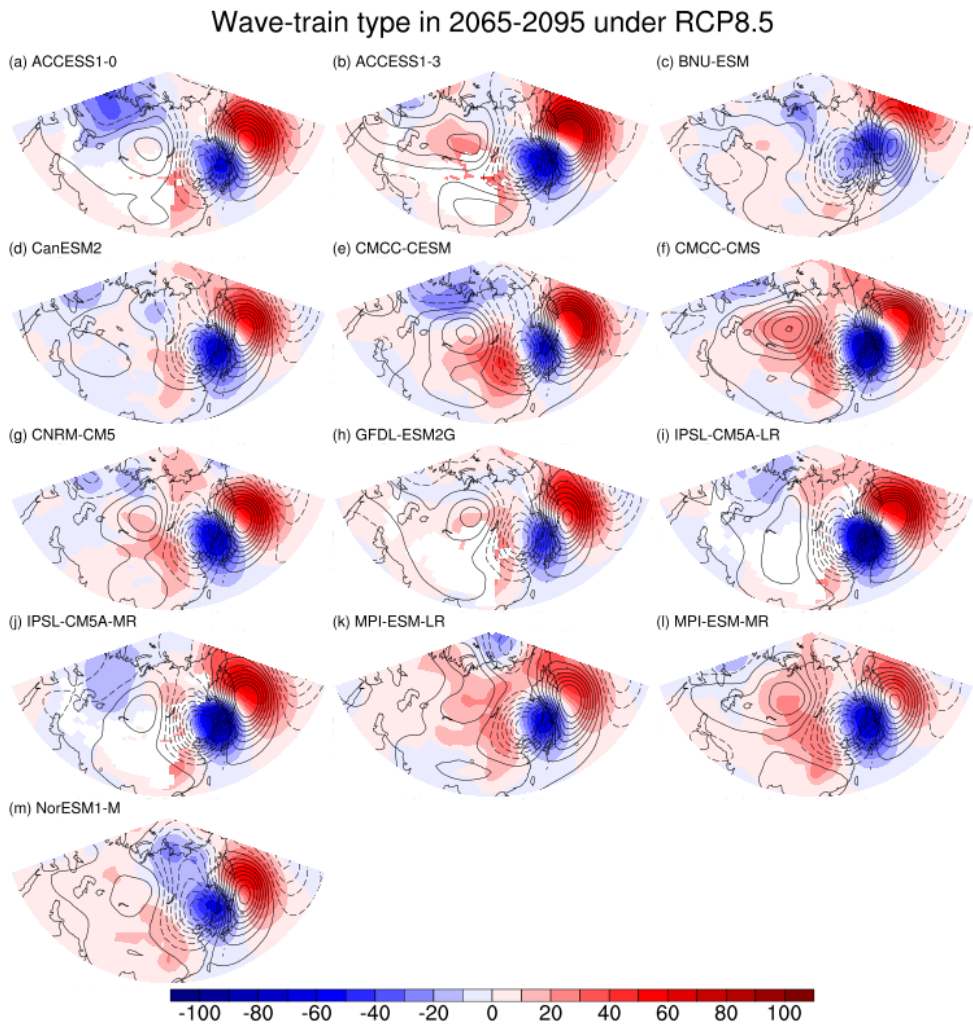

Figure 12. Same as Figure 8 but under RCP8.5 for 2065-2095.

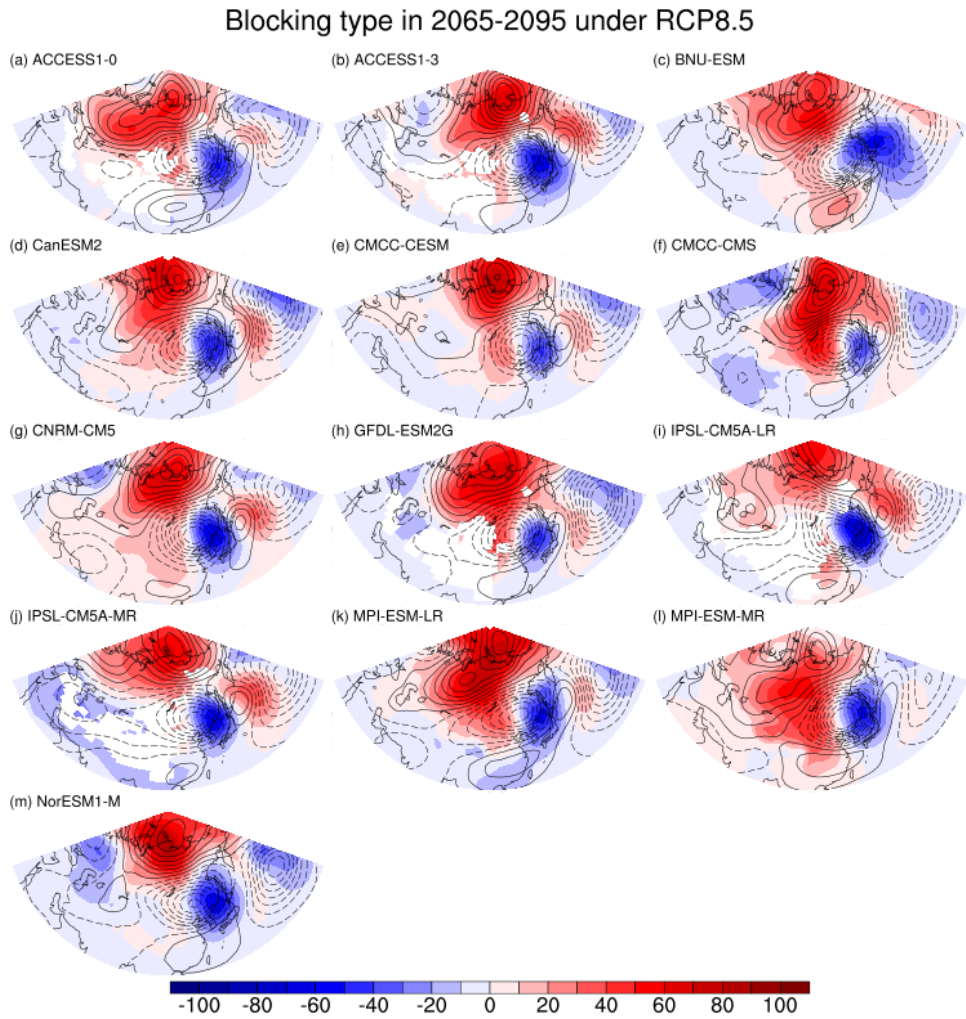

Figure 13. Same as Figure 8 but of the blocking type under RCP8.5 for 2065-2095.

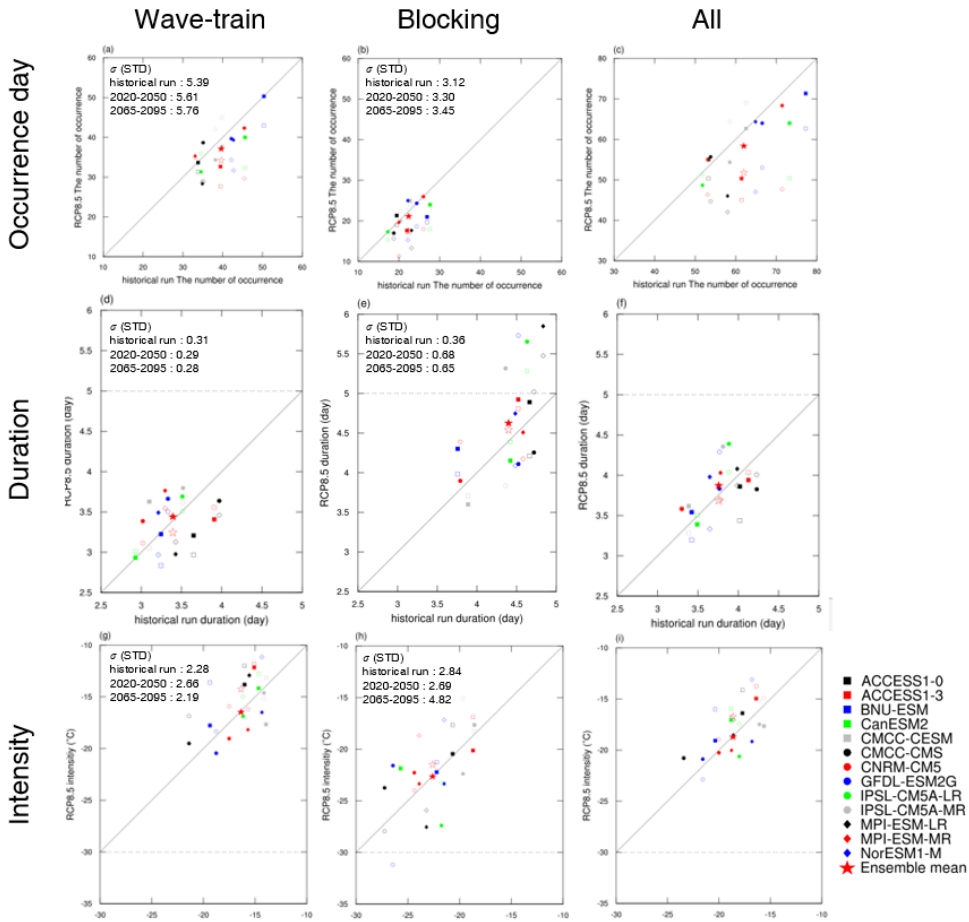

Figure 14. Scatter plot of the occurrence day (per decade), duration, and intensity. Close markers is for 2020-2050 and Open markers are for 2065-2095.

5. Summary & discussion

In this study the new method for classification is introduced. In the index methods potential temperature on 2 PVU (dynamical tropopause) is used to define the wave-train index and the blocking index. The potential temperature is conserved in adiabatic process and it is used to define Northern Hemisphere blocking in Pelly and Hoskins (2003). We used this variable to capture upper wave-train type and meridional dipole structure in blocking type. The wave-train index is defined difference between potential temperature anomalies on 2 PVU averaged over the western North Pacific and over northeast China. On the other hand, the blocking index is defined the difference between potential temperature anomalies over subarctic and over northeast China.

The index method is used to classify cold surges in observation to confirm the performance of it. The wave-train (blocking) type cold surge is identified when the WI (BI) larger than zero and larger than BI (WI). The 188 cold surges are the wave-train cold surge which have baroclinic growing wave with southeastward expansion of Siberian high. The 104 cold surges of the blocking type have meridional dipole structure with barotropic blocking over the subarctic region and baroclinic trough over East Asia with southward expansion of Siberian high. The blocking type cold surge is less frequent bur it is longer and stronger than the wave-train type. The index method well classifies cold surges in observation.

The present paper examined the changes of cold surge using the index method to classify cold surges into wave-train type and blocking type in the future climate. We use 13 CGCMs in CMIP5 under RCP8.5 to examine the cold surge in the future climate. The simulated wave-train type cold surge shows baroclinic wave and the

simulated blocking type cold surge shows positive geopotential height anomaly in subarctic and meridional dipole structure. The simulated blocking type is longer and stronger than wave-train type likewise the observation. The index method successfully classifies two types in CGCMs. However the spatial pattern is stronger and every CGCM simulates less occurrence day, stronger intensity in both type than observation. In conclusion the index method works in CGCMs but there is bias in simulating characteristics.

The duration of RCP8.5 is from 2006 to 2100 which is not one climate so we divide 2 period; the early twenty one century (2020-2050) and the late twenty one century (2065-2095). The spatial pattern of the early and late twenty one century shows the general feature of each cold surge. However the characteristics changes in the future climate. The occurrence day decreases in the most of CGCMs in both types. The duration decreases in the wave-train type and increases in the blocking type in the ensemble mean. The intensity in both type decline but magnitude is larger in the wave-train type than the blocking type in addition to 10% strongest cold surge decreasing. However the change of duration and intensity in each CGCM has large variation. The intensity is defined by the sum of temperature during cold surge duration so we calculated averaged intensity. The decrease of duration and warmer temperature anomaly than historical in the wave-train type leads to weaker cold surge. Although the duration of the blocking type increases the blocking type weaken due to warmer temperature anomaly.

The decrease of occurrence day in both type is clear. By definition of the cold surge, temperature variability and Siberian high influence on the change of the cold surge. In this study temperature variability in historical run is used for definition of

the cold surge. Thus the change of temperature variability influences the occurrence day of cold surge. The occurrence of cold surge may be closely related to Siberian high amplification. The decrease of Siberian high amplification indicates the decrease of occurrence day also the Jet weakening can be one of reasons. This part will be studied in next study.

It is cautionary that only first ensemble member of CGCMs is analyzed which might reduce confidence of results due to the model-generated atmospheric internal variability. Next, the large spread in the duration of the simulated blocking type cold surge indicates limitation of the performance of the CGCMs. Some CGCMs especially simulate large change of duration over 1.6 day in the blocking type. There may be factors which influence this change of cold surge. It is guessed that some factor in CGCMs have large variation model-to-model. This aspect will be studied to improve the performance of model simulation.

6. Reference

Baldwin MP, Dunkerton TJ (1999) Propagation of the Arctic Oscillation from the stratosphere to the troposphere. J Geophys Res-Atmos **104**(D24):30937-30946.

Chen TC, Yen Mc, Huang WR, Gallus WA (2002) An East Asian cold surge: case study. Mon Weather Rev **130**(9):2271-2290.

Cohen J, Satio K, Entekhabi D (2001) The rold of the Siberian high in Northern Hemisphere climate variability. Geophys Res Lett **28**(2):299-302.

Dee DP, Uppala SM, Simmons AJ, Berrisford P, Poli P, Kobayashi S, Andrae U, Balmaseda MA, Balsamo G, Bauer P, Bechtold P, Beljaars ACM, van de Berg L, Bidlot J, Bormann N, Delsol C, Dragani R, Fuentes M, Geer AJ, Haimberger L, Healy SB, Hersbach H, Holm EV, Isaksen L, Kallberg P, Kohler M, Matricardi M, McNally AP, Monge-Sanz BM, Morcrette JJ, Park BK, Peubey C, de Rosnay P, Tavolato C, Thepaut JN, Vitart F (2011) The ERA-Interim reanalysis: configuration and performance of the data assimilation system. Q J Roy Meteor Soc **137** (656):553-597. doi:10.1002/QJ.828.

Ding Y, Krishnamurti TN (1987) Heat-budge of the Siberian high and the winter monsoon. Mon Weather Rev **115**(10):2428-2449.

Hoskins BJ, Mcintyre ME, Roberton AW (1985) On the use and significance of isentropic potential vorticity maps. Q J Roy Meteor Soc **111**(470):877-946.

Hoskins BJ, Berrisford (1988) A potential vorticity view of synoptic development. Meteorol Appl 4(4):325-334. doi:10.1017/s1350482797000716.

Jeong CH, Hitchman MH (1982) On the role of successive downstream development

in East Asian Polar air outbreaks. Mon Weather Rev **110**(9):1224-1237.

Jeong J-H, Ho C-H (2005) Changes in occurrence of cold surges over East Asia in association with Arctic Oscillation. Geophys Res Lett 32:L14704. doi:10.1029/2005GL023024.

Jeong J-H, Kim B-M, Ho C-H, Chen D, Lim G-H (2006) Stratospheric origin of cold surge occurrence in East Asia. Geophys Res Lett **33**:L14710. doi:10.1029/2006/GL026607.

Kalkstein LS, Tan GR, Skindlov JA (1987) An Evaluation of 3 Clustering Procedures for Use in Synoptic Climatological Classification. J Clim Appl Meteorol **26** (6):717-730

Peings Y, Cattiaux, H. Douville (2013) Evaluation and response of winter cold spells over Western Europe in CMIP5 models. Clim Dynam **41** (11-12) 3025-3037. doi:10.1007/s00382-012-1565-z.

Park T-W, Jeong J-H, Ho C-H, Kim S-J (2008) Characteristics of atmospheric circulation associated with cold surge occurrences in East Asia: a case study during 2005/06 winter. Adv Atmos Sci **25**(5): 791-804. doi:10.1007/s00376-008-0791-0.

Park T-W, Ho C-H, Yang S, Jeong J-H (2010) Influences of Arctic Oscillation and Madden Oscillation and Madden-Julian Oscillation on cold surges and heavy snowfalls over Korea: a case study for the winter of 2009-2010. J Geophys Res-Atmos **115**:D23122. doi:10.1029/2010JD014794.

Park T-W, Ho C-H, Yang S (2011) Relationship between the Arctic Oscillation and cold surges over East Asia J Clim **24**(1):68-83. doi:10.1175/2010jcli3529.1.

Park T-W, Ho C-H, Deng Y (2014) A synoptic and dynamical characterization of

wave-train and blocking cold surge over East Asia. Clim Dynam **43** (3-4):753-770. Doi:10.1007/s00382-013-1817-6.

Pelly JL, Hoskins BJ (2003) A new perspective on blocking. J Atmos Sci 60(5):743-755.

Takaya K, Nakamura H (2005a) Mechanisms of intraseasonal amplification of the cold Siberian high. J Atmos Sci **62**(12): 4423-4440.

Takaya K, Nakamura H (2005b) Geographical dependence of upper level blocking formation associated with intraseasonal amplification of the Siberian high, J Atmos Sci **62**(12): 4441-4449.

Thompson DWJ, Wallace JM (1998) The Arctic Oscillation signature in the winter time geopotential height and temperature fields. Geophys Res Lett **25**(9):1297-1300.

Tibaldi S, Monlteni F (1990) On the operational predictability of blocking. Tellus **42A**:343-365.

Tyrlis E, Hoskins BJ (2008) The morphology of Northern Hemisphere blocking. J Atmos Sci **65** (5):1653-1665. doi:Doi 10.1175/2007jas2338.1

Woo S-H, Kim B-M, Jeong J-H, Kim S-J, Lim G-H (2012) Decadal changes in surface air temperature variability and cold surge characteristics over northeast Asia and their relation with the Arctic Oscillation for the past three decades (1979-2011). J Geophys Res, **117**, D18117, doi:10.1029/2011JD016929

Zhang Y, Sperber KR, Boyle JS (1997) Climatology and interannual variation of the East Asian winter monsoon: Results from the 1979-95 NCEP/NCAR reanalysis.

Mon Weather Rev **125** (10):2605-2619.

국문초록

동아시아 한파는 역학적 특징에 따라 웨이브 트레인 한파와 블로킹 한파로 분류할 수 있다. 본 연구에서는 웨이브 트레인, 블로킹 한파를 분류하기 위해 두가지 지수를 고안하였다. 두 지수는 2PVU (2 잠재 소용돌이 단위) 면의 온위를 사용하여 상층 웨이브 트레인 패턴과 남북방향의 쌍극 구조를 잡아내기 위해 고안되었다. 웨이브 트레인 지수는 웨이브 트레인 형태 중 서태평양의 양의 아노말리와 북동 중국의 양의 아노말리가 나타나는 점을 이용하여 두 지역의 2PVU 면의 온위 아노말리 차이를 이용하여 정의하였다. 블로킹 지수는 쌍극구조인 아북극지역의 양의 아노말리, 중국 북동부 지역의 음의 아노말리가 나타나는 점을 이용해 두 지역의 2PVU 면의 온위 아노말리 차이를 이용하여 정의하였다. 두 종류의 한파는 주요한 특징을 갖는다. 웨이브 트레인 한파의 경우 시베리아 고기압의 남동방향의 확장과 함께 경압성 웨이브가 나타나며 블로킹 한파의 경우 시베리아 고기압이 남쪽으로 확장하며 아북극지역의 블로킹과 동아시아 몬순 골의 강화가 나타난다. 두 한파의 특징으로는 블로킹 한파가 웨이브 트레인 한파보다 강도가 강하고 기간이 길지만 발생횟수가 더 적다. 본 연구에서는 웨이브 트레인, 블로킹 형태를 가지지 않은 경우 한파 분류에서 제외하였다.

지수 방법을 CMIP5의 13개 모델에 적용한 결과 웨이브 트레인, 블로

킹 한파가 잘 분류되었다. 관측과 마찬가지로 웨이브 트레인 한파는 웨이브 트레인 형태가 나타나며 블로킹 한파는 쌍극구조가 잘 나타났다. 하지만 관측과 히스토리컬 런의 결과를 비교할 경우 대부분의 CMIP5 모델은 한파 발생횟수를 적게, 강도는 강하고 기간을 길게 모의하고 있었다. RCP8.5 시나리오에서는 두 종류의 한파 모두 앙상블 평균 발생횟수는 감소와 강도의 약화가 보였다. 반면 기간은 블로킹 한파는 증가하고 웨이브 트레인 한파는 감소하였다.

주요어: 한파, 동아시아, 분류, CMIP5

학번: 2013-20348